agriculture

MDPI

Article

Development of a Real-Time Tractor Model for Gear Shift Performance Verification

Gyuha Han [1], Da-Vin Ahn [1,2], Doyeop Kwon [1], Heung-Sub Kim [3], Young-Jun Park [1,2,4,*] and Jin Woong Lee [5,*]

[1] Department of Biosystems Engineering, Seoul National University, Seoul 08826, Republic of Korea; letfree612@snu.ac.kr (G.H.); mt1125@snu.ac.kr (D.-V.A.); kwondoyeop@snu.ac.kr (D.K.)
[2] Convergence Major in Global Smart Farm, Seoul National University, Seoul 08826, Republic of Korea
[3] Department of Smart Industrial Machine Technologies, Korea Institute of Machinery and Materials, Daejeon 34103, Republic of Korea; subkim@kimm.re.kr
[4] Research Institute of Agriculture and Life Science, Seoul National University, Seoul 08826, Republic of Korea
[5] Smart Agricultural Machinery R&D Group, Korea Institute of Industrial Technology, Gimje 54325, Republic of Korea
* Correspondence: yjpark95@snu.ac.kr (Y.-J.P.); reallybear@kitech.re.kr (J.W.L.)

Abstract: Verification of the system is essential during the development of a tractor; however, there are cost and time limitations when verification is performed on an actual tractor. To solve this problem, we developed a tractor model for real-time simulation to verify the gear shift performance of the tractor and evaluate the control algorithm. This study examined and modeled a dual-clutch transmission (DCT)-type 105 kW class tractor. The proportional control valve, synchronizer, and clutch were modeled to accurately implement the shift behavior, and the developed individual model was verified based on actual individual product test data. The 45 s driving simulation was conducted to confirm whether real-time simulation of the entire developed tractor model was possible and whether it simulated the behavior of the target tractor well. The driving simulation results confirmed that the driving speed of the tractor model matched the engine speed, transmission gear ratio, and tractor specifications, and the gear shift performance of the tractor model according to the number of gears was confirmed. The simulated model thus satisfies the characteristics of the target tractor and can be used to verify the gear shift performance, indicating that the model can verify the performance of the control algorithm in real time.

Keywords: gear shift performance; tractor simulation model; real-time simulation; dual-clutch transmission

Citation: Han, G.; Ahn, D.-V.; Kwon, D.; Kim, H.-S.; Park, Y.-J.; Lee, J.W. Development of a Real-Time Tractor Model for Gear Shift Performance Verification. *Agriculture* **2023**, *13*, 2133. https://doi.org/10.3390/agriculture13112133

Academic Editors: Galibjon M. Sharipov and Kenshi Sakai

Received: 8 October 2023
Revised: 10 November 2023
Accepted: 10 November 2023
Published: 12 November 2023

1. Introduction

Agricultural tractors are composed of a mechanical system that creates and transmits power and a control system that makes the elements of each mechanical system operate for the desired purpose. The mechanical systems in newly developed tractors include elements used in existing tractors and elements developed to implement new functions. These elements must be tested and verified at the component level to determine their suitability for mechanical system configurations. In addition to each element being developed and verified part-by-part, the components that are connected to enable systematic operation should be verified during the tractor development process. Additionally, the control system should be connected to the mechanical system and verified during tractor development. However, when verification of the control system is performed on a real tractor, there is a limitation in that costs increase depending on the system's reliability. In addition, considering the time required for verification in the real tractor, verification through simulation is reasonable.

Recently, many studies have been conducted using simulation models to develop and verify tractor mechanical and control systems. Cheng et al. [1] developed a full-tractor simulation model, including the control system, using MATLAB and Carsim to improve the performance of the electronic stability program system among the tractor control systems. Mao et al. [2] used Modelica to build a drive system model for an electric tractor and predicted its performance. Yiwei et al. [3] built a power-shift transmission (PST) model, including mechanical, hydraulic, and control systems, using Adams, AMEsim, and MATLAB to develop a new type of tractor. Li et al. [4] built a tractor simulation model, including a driver and mechanical system, using MATLAB to develop and verify the automatic starting control of a tractor. Baek et al. [5] built a tractor simulation model, including a transmission and control system, using Simulation X to develop an electric all-wheel drive tractor. Kumar et al. [6] built the electro-hydraulic hitch control valve model of agricultural tractors to implement a hydraulic system to dynamic simulation models. Jeon et al. [7] developed a 3D tractor-driving simulator to verify the performance of a coverage path planner for auto-guided agricultural machines. Watanabe et al. [8] used a driving simulator with a motion system to identify the overturning scenarios of a tractor. Mocera [9] developed a tractor electric system model to test the performance of the energy management strategy for parallel hybrid electric tractors. The tractor simulation models built in existing studies were developed only for performance analysis simulation and not for real-time performance prediction simulation. The offline simulation model developed for a performance analysis enables a detailed analysis tailored for development purposes through sophisticated modeling. However, the offline simulation model cannot be used as a plant model for control algorithm verification because it cannot operate in real time. The simulation model, which can operate at the same rate as clock time without the occurrence of overruns, is called a real-time simulation model. It computes all internal state equations and functions in a shorter time than the simulation time-step during a discrete time simulation with a constant step and simulates the behavior similar to an actual system within the scope of real-time operation. It allows for the system's operation to be confirmed in real time, allowing for the performance and stability to be evaluated, and is mainly used to verify control algorithms. Additionally, the operation of an actual system can be simulated quickly, allowing for research to be conducted more efficiently [10]. Because of the advantages that real-time simulation has over offline simulation, this study developed a tractor model for real-time simulation to predict the performance of not only the control system, but also the mechanical system to verify the gear shift performance and evaluate the stability of the tractor.

Research using real-time simulation is being conducted during the development and verification of vehicles. Ruan et al. [11] created a powertrain model for real-time simulation and performed hardware-in-the-loop simulation to develop energy-saving controls for HEV. Tamas et al. [12] used MATLAB/Simulink to model an EV propulsion system as a vehicle dynamic model for real-time simulation. Moten et al. [13] created a real-time multibody model that satisfies the dynamic characteristics for designing and verifying advanced driver assistance systems (ADAS). Abdelrahman et al. [14] modeled a motor and controller for a real-time simulation to develop an EV powertrain. Aksjonov et al. [15] created a real-time vehicle model with 14 degrees of freedom using IPG CarMaker to verify the control method of an electrohydraulic antilock braking system. Parra et al. [16] built the real-time multibody vehicle models that satisfy development capabilities by C code. Moreno et al. [17] used MATLAB/Simulink to develop the real-time agricultural robot model to validate the path-tracking strategy. Liu et al. [18] built the real-time hybrid electric vehicle model to validate a speed planning and energy management strategy. Yang et al. [19] used OPAL-RT and MATLAB/Simulink to develop a nonlinear real-time electric vehicle model that included a drive system, battery system, and control units. Although many studies have been conducted to produce and validate a real-time simulation model according to the specific purpose of the vehicle, no studies have been conducted on models driven in real time while finely simulating the mechanical systems involved in gear shift performance. Improving gear shift performance is directly related to the ride comfort of the vehicle, making it one of the key factors in vehicle development [20–22]. The gear shift performance varies depending on the synchronization time of speed and torque generated through the clutch and synchronizer during the gear shift process [23–25]. If the shaft torque variation that occurs during the tractor's shifting process is prolonged, the driver can feel uncomfortable. Since synchronization time varies depending on shift control, the model that can validate shift performance according to shift control is needed.

In this study, a tractor model designed for real-time simulation was developed in detail to accurately replicate the behavior of a mechanical system involved in gear shifting. The main objective of this study is to develop a plant model for verifying control algorithms in the tractor development process. One of the primary goals during tractor development process is to reduce time resource consumption. To achieve this goal, the control algorithms must be finalized before the tractor development phase. This enables the integration of verified control algorithms directly into the actual tractor, reducing the overall development timeline. In this study, the real-time plant model that enables real-time response and precision for the actual tractor was developed to verify the control algorithm, rather than merely replicating the behavior of the actual tractor. To accomplish this, detailed submodels were developed through the verification process for pre-selected and developed components that constitute the entire plant model. This approach, involving the verification of components and the overall model operation in the tractor development process, allowed us to build a plant model specifically for the verification of control algorithms.

In instances where the actual tractor development has been completed, developing the plant model for verifying control algorithms becomes redundant, as the focus shifts directly to the actual tractor. However, this development process involves several stages, consuming considerable time resources. Therefore, the presented methodology involved verifying each component and confirming the operation of the plant model during the tractor development process. A target system was selected to develop the tractor simulation model, and its characteristics were reflected in the model. The model of the synchronizer, clutch, and pressure control valve, which is involved in shifting while driving, was built in detail within the scope of a real-time simulation and verified from individual test results. The developed tractor model (plant model) was confirmed through a driving simulation to determine whether it could be performed in real time and whether the gear shift performance could be validated.

In summary, the main significance and innovation of this study are as follows:

- A real-time plant model ensuring real-time responsiveness and high precision of the actual tractor to be developed was developed to verify control algorithms in the tractor development process.
- In order to evaluate the shifting performance of control algorithms accurately, detailed modeling of shifting-related components was developed and validated from the test results.
- The entire plant model was validated through driving simulation to confirm the real-time simulation capability and suitability for verifying control algorithms.

2. Materials and Methods

2.1. Target Tractor

The target tractor modeled in this study was a 105-kW dual-clutch transmission (DCT)-type tractor. The specifications of the target tractor used in the model are listed in Table 1.

The DCT is a transmission system consisting of two clutch sets, and each clutch set operates in connection with odd and even gears [26]. Figure 1 shows the DCT system of the target tractor used in this study. The two clutch sets operate independently, and each clutch set is used alternately to engage the next gear while driving. The shifting process of the DCT system is performed as follows: When switching from the current gear to the next target gear, the first clutch is disengaged. When the first clutch is disengaged, the gear connected to the second clutch is also disengaged, and the target gear is engaged in the second clutch. After the connection, the second clutch is engaged, and shifting is completed. The model was designed to reflect the characteristics of the DCT.

Table 1. Specification of target tractor used in this study.

Item	Specification
Model	DCT type tractor
Power	105 kW
Rated engine speed	2300 RPM
Max engine torque	600 Nm
Mass	5000 kg
Rear wheel radius	0.835 m
Speed	0~40 km/h

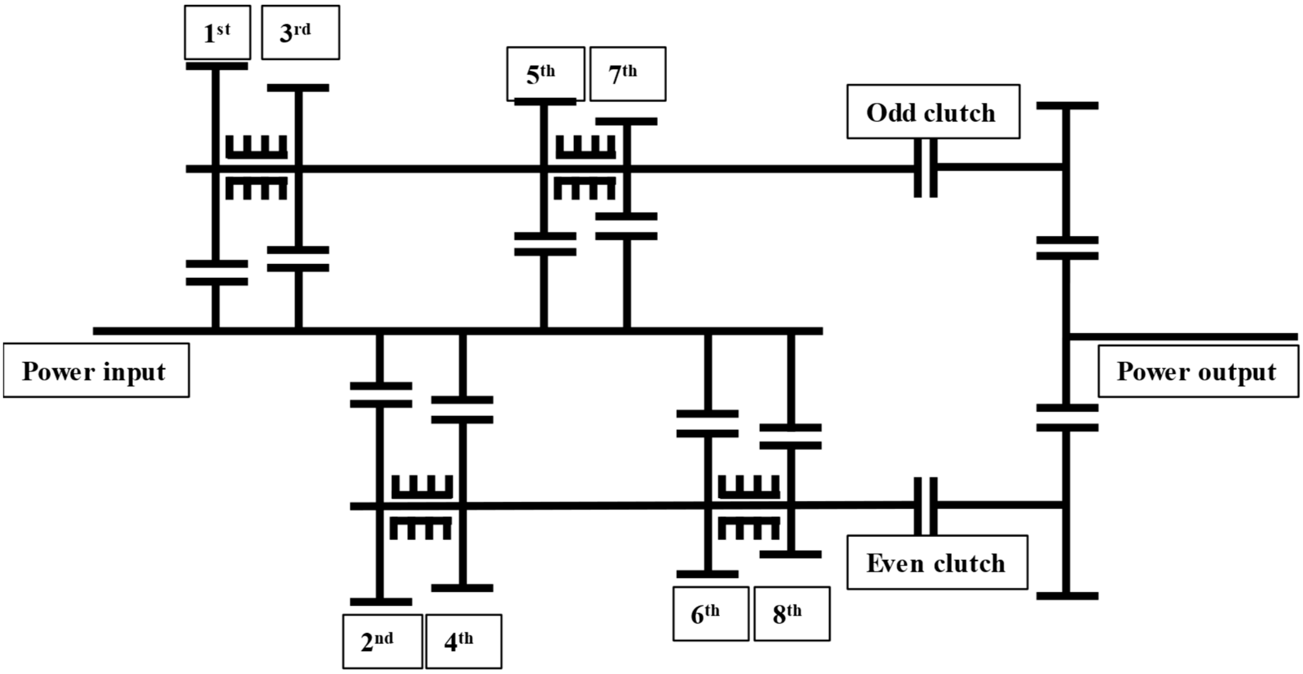

Figure 1. Schematic diagram of DCT used in the target tractor.

2.2. Model Outline

In this study, a tractor simulation model was developed using MATLAB/Simulink based on a dual-clutch transmission-type tractor. The gear shift process of the DCT is divided into two phases: a torque phase, in which torque is transmitted, and an inertia phase, in which speed changes. In this process, speed synchronization occurs through a clutch and synchronizer [27,28]. Song et al. [29] developed a DCT model that implemented a clutch damper to validate the DCT gear shift process. Galvagno et al. [30] developed the DCT dynamic model that implemented the influence of synchronizers. Referring to previous research, detailed modeling of clutches and synchronizers is essential in order to evaluate the control algorithm to confirm and improve the shift shock of tractors with DCT systems. In this study, the clutch and synchronizer, which greatly affect the gear shift performance of the DCT system, were simulated in detail, and the proportional control valve that supplies pressure for engaging and disengaging the clutch and synchronizer was also modeled in detail. Figure 2 shows an outline of the tractor model. The input data of the tractor model for implementing shift performance can be divided into three types. The driver interface (DI) is the signal input by the driver, and a description of each signal is provided in Table 2. Transmission exchange (TX) is a signal used to control each sub-model, and a description of each signal is presented in Table 3. The plant model (PM) receives feedback from the data output of the model to control it according to its current state. The data output from the model is the signal output from each submodel, and a description of each signal is provided in Table 4.

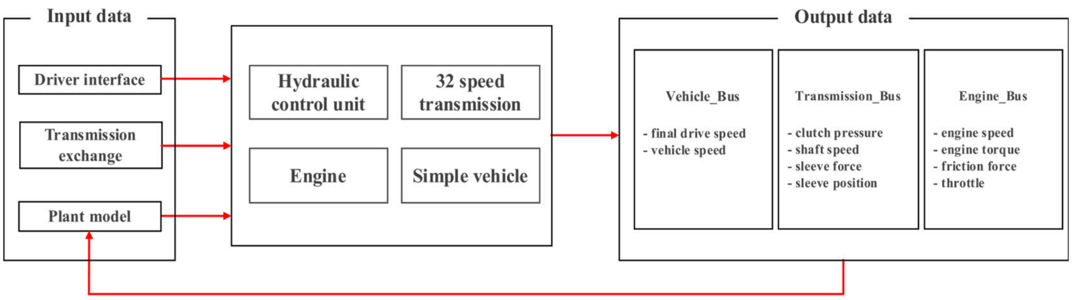

Figure 2. Outline of simulation model.

Table 2. Description of driver interface signals.

Input Signal	Description
Norm brake	Brake torque by brake pedal
Gradient	Gradient of the ground
Upshift	Driver pressing the upshift button
Downshift	Driver pressing the downshift button
Oil temperature	Oil temperature of hydraulic system
System pressure	System pressure of the hydraulic system

Table 3. Description of transmission exchange signals.

Input Signal	Description
Sync1 current	Synchronizer pressure control valve (PCV) 1 control current
Sync2 current	Synchronizer PCV 2 control current
Sync3 current	Synchronizer PCV 3 control current
Sync4 current	Synchronizer PCV 4 control current
Sync5 current	Synchronizer PCV 5 control current
Sync6 current	Synchronizer PCV 6 control current
Sync7 current	Synchronizer PCV 7 control current
Sync8 current	Synchronizer PCV 8 control current
Creep	Creep shift dog clutch control signal
Low	Low shift dog clutch control signal
Middle	Middle shift dog clutch control signal
High	High shift dog clutch control signal
FWD clutch current	Forward clutch PCV control current
REV clutch current	Reverse clutch PCV control current
Odd clutch current	Odd clutch PCV control current
Even clutch current	Even clutch PCV control current
Key	Engine key mode
Target speed	Engine target speed

Table 4. Description of plant model output data.

Output Signal	Description
Engine throttle	Throttle output from the engine model
Engine speed	Speed output from the engine model
Engine torque	Torque output from the engine model
Friction torque	Engine friction torque output from the engine model
Clutch pressure	Clutch pressure output from the Hydraulic control unit (HCU) model
Sleeve force	Synchronizer actuator sleeve force output from the HCU model
Sleeve position	Synchronizer actuator sleeve position output from the 32-speed transmission model

Table 4. *Cont.*

Output Signal	Description
Shaft speed	Shaft speed output from the 32-speed transmission model
Vehicle speed	Vehicle speed output from the simple vehicle model
Final drive speed	Final drive speed output from the simple vehicle model

The model consisted of four submodels that simulated the tractor's mechanical and control systems. The hydraulic control unit (HCU) model controlled the pressure and force supplied to the 32-speed transmission's clutch, synchronizer, and manual range shift according to the current input. The engine model transmitted power through a 32-speed transmission according to engine operating status and target speed. The 32-speed transmission model was a 32-speed transmission with an odd and even clutch in a dual-clutch transmission and an 8-speed main shift without power interruption that used a hydraulic actuator and a manual 4-speed range shift. The model transferred the power received from the engine to the final drive of the simple vehicle model according to the HCU control signal. The simple vehicle model was a dynamic model that calculated the speed and acceleration of the tractor based on the transmitted power. Figure 3 is an illustration of the entire model with four submodels connected.

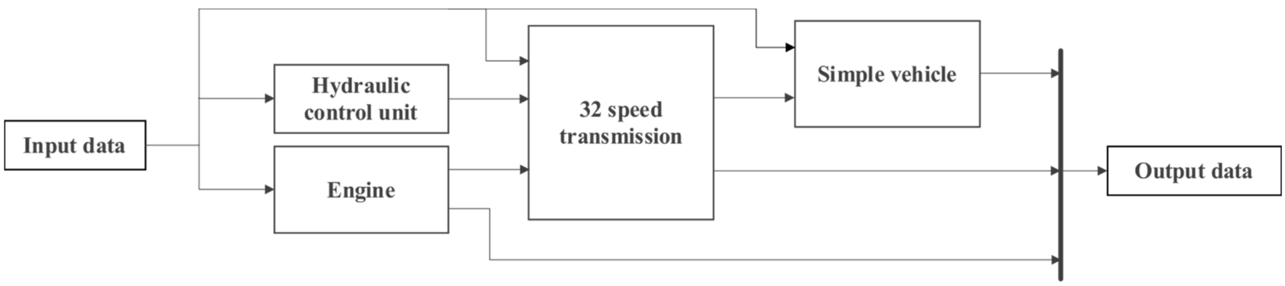

Figure 3. Figure of the full simulation model.

2.3. HCU Modeling

The hydraulic control unit (HCU) is a module that supplies hydraulic pressure to the transmission according to the current input signal. To implement these HCU functions in the tractor model, a clutch proportional control valve (PCV), synchronizer actuator, and dog clutch pressure were modeled. Figure 4 shows a schematic of the HCU modeling. The clutch PCV supplied pressure for clutch engagement according to the current input signal, and four valves were modeled: one each for the forward, reverse, odd, and even clutches. The synchronizer actuator was implemented with a proportional control valve that supplied pressure to both ends of the actuator according to the current input signal and an actuator that supplied the sleeve force to fasten the synchronizer according to the supplied pressure. Four units of synchronizer actuators (1–3 stage, 2–4 stage, 5–7 stage, 6–8 stage) were modeled using two proportional control valves and an actuator. Dog clutch pressure models were built with four models, one for each sub-shift gear, to supply pressure to the range-shift dog clutch through the mechanical shift signal input by the driver.

Hydac PDR10830 was selected as the model target for the clutch PCV modeling. PDR 10830 is the model name of a proportional control valve. Figure 5a shows the current–pressure characteristics of the valve provided by the manufacturer's (Hydac) catalogue. Single-valve tests were performed to reflect the static and dynamic characteristics of PDR10830 in modeling. A ramp-response test was conducted to confirm the static characteristics of the PCV, which were the control pressure characteristics of the input current of the target proportional control valve. The ramp-response test measures the current input value and control pressure by adjusting the ramp input of the maximum current of 1400 mA by 1 round trip at a speed without dynamic influence (rising and falling time of 20 s) at a supply pressure of 35 bar, supply flow rate of 9 L/min, and starting temperature of 46 °C. Figure 5a shows the results of the ramp-response test. When compared to the current–pressure characteristic curve of the valve catalog, it was confirmed that the single-valve test results showed a very small error and followed the catalog well. A step-response test was conducted to confirm the dynamic characteristics of the PCV, that is, the pressure rise time in response to the input current of the PCV. The step-response test measured the control pressure by providing a step input from 0% to 100% of the maximum control pressure during a maintenance and release period of 5 s, where the control pressure was sufficiently stable. Figure 5b shows the results of the step-response test used to confirm the dynamic characteristics. The test results confirmed that the rise time required to reach 90% of the maximum control pressure of the PCV was 0.25 s.

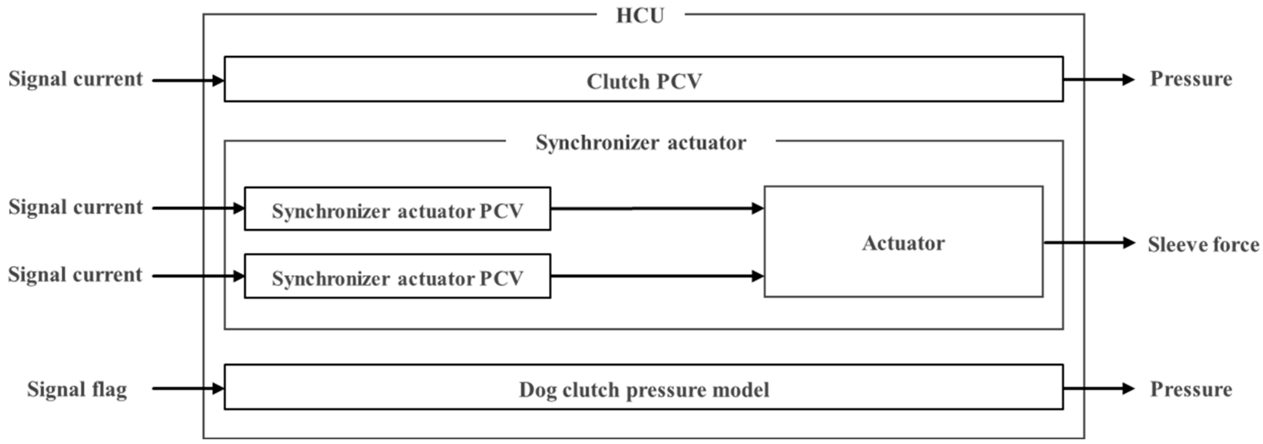

Figure 4. Outline of the HCU model.

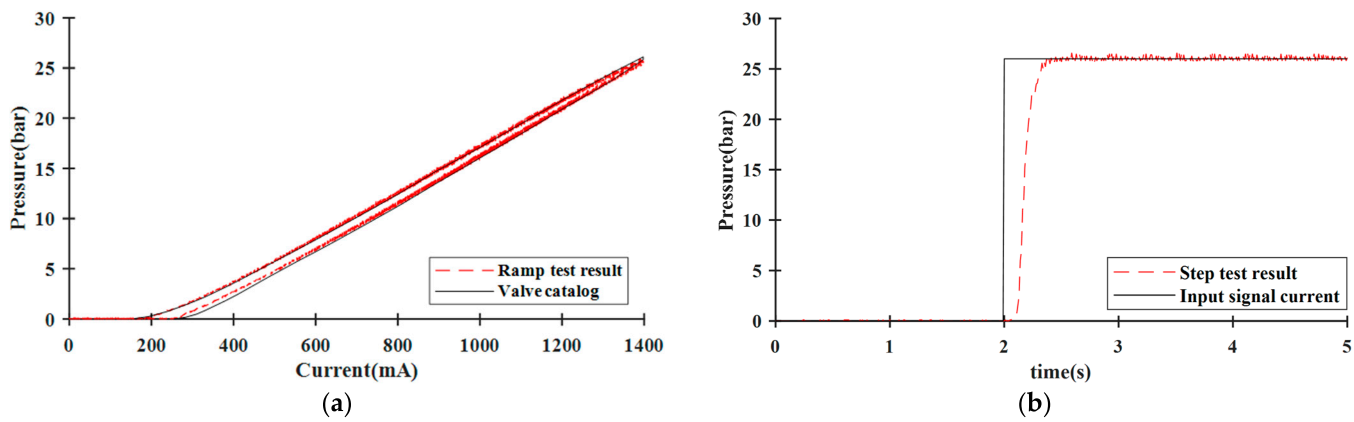

Figure 5. PDR10830 test data: (**a**) Ramp test data; (**b**) Step test data.

Figure 6 shows the clutch PCV model, which reflects the static and dynamic characteristics of the target valve. The current–pressure characteristics of the ramp-response test results were used in table-based modeling to reflect the static characteristics of the model. A transfer function based on step-response test results was used to reflect the dynamic characteristics of the model. The pressure calculated from the clutch PCV model was supplied to the clutch model of the 32-speed transmission.

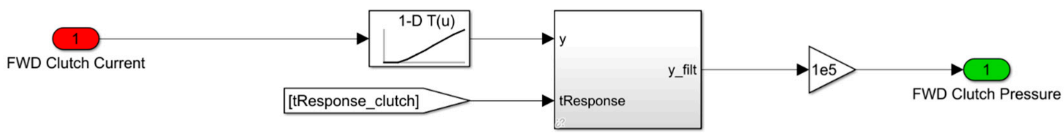

Figure 6. Clutch PCV model.

To verify whether the clutch proportional control valve model simulated the target proportional control valve well, the same ramp and step-response tests as the single valve test that were performed with the target proportional control valve were performed. Figure 7a,b compare test results and simulation results for the valve model's ramp response and step response, respectively. It was confirmed that the model's ramp-response simulation results showed good linearity and simulated the static characteristics of the target proportional control valve reflected in the modeling well. The error of 0.005 s between the model's rise time and the target proportional control valve rise time obtained through the step-response simulation was smaller than 0.01 s, which was that of the cycle of the tractor HCU operating at 100 Hz. This means that the dynamic characteristics of the control valve have been well simulated.

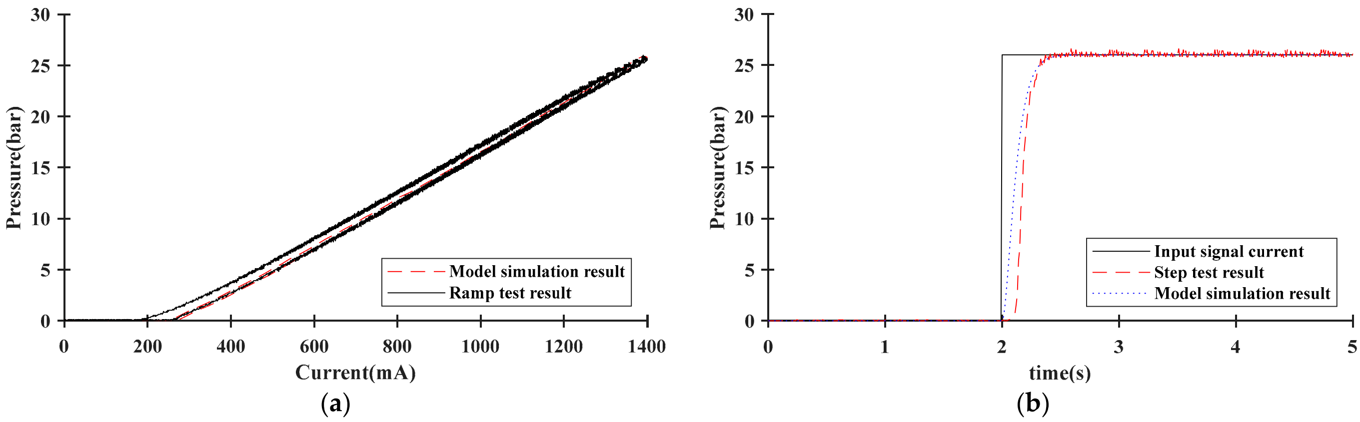

Figure 7. Clutch PCV model simulation data compared with valve test data: (**a**) Ramp test data; (**b**) Step test data.

The synchronizer actuator model consisted of two proportional control valves and one actuator. For example, a 1–3 stage synchronizer actuator consists of a 1-stage synchronizer proportional control valve, a 3-stage synchronizer proportional control valve, and a 1–3 stage actuator. The pressure supplied by the two proportional control valves was input to the actuator, and the synchronizer actuator sleeve force was calculated based on the cross-sectional area and sleeve position. Hydraforce EHPR-G38A was selected as the model target for synchronizer proportional control valve modeling. EHPR-G38A is the model name of a proportional control valve. Figure 8a shows the current–pressure characteristics of the valve provided by the manufacturer's (Hydraforce) catalogue. Similar to the clutch proportional control valve, a single-valve test was conducted to verify the characteristics of the target valve for synchronizer proportional control valve modeling. Figure 8a shows the ramp-response test results. Compared with the current–pressure characteristic curve of the valve catalog, it was confirmed that a very small error was observed in the current range of 400–1000 mA, but the reactivity of the valve did not follow the catalog in the current range of 200–400 mA. It was determined that the ramp-response test results could be used to model the proportional control valve because a current between 500 and 900 mA was input into the synchronizer for gear shift control. Figure 8b shows the results of the step-response test and confirms that the rise time is 0.11 s.

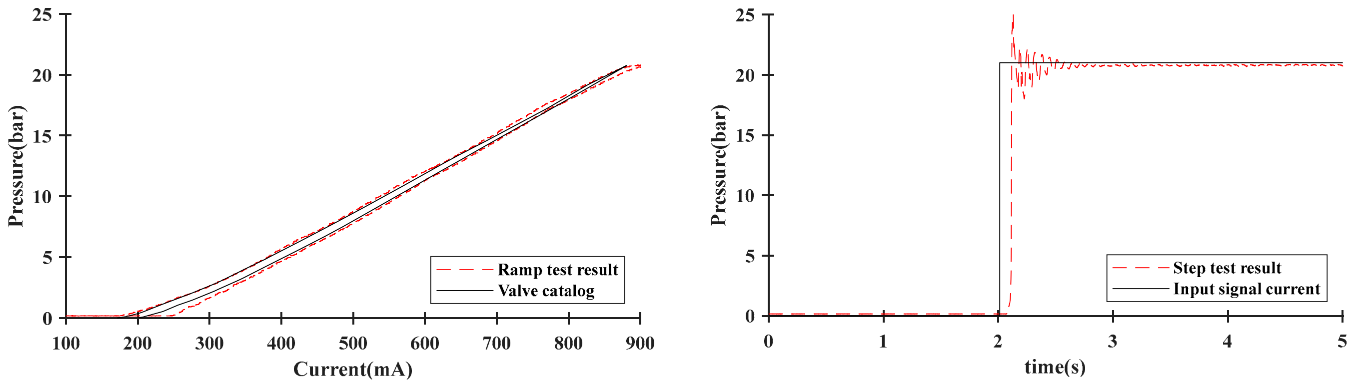

(**a**) (**b**)

Figure 8. EHPR-G38A PCV test data: (**a**) Ramp test data; (**b**) Step test data.

The synchronizer proportional control valve was modeled using the results of the ramp and step-response tests as the clutch proportional control valve in Figure 6, and the pressure calculated in the model was modeled to be supplied to the actuator model. The synchronizer proportional control valve model was verified as identical to the clutch proportional control valve. Figure 9a compares the ramp-response test results and synchronizer PCV model simulation results. Figure 9b compares the step-response test results and the synchronizer PCV model simulation results. Similar to the clutch PCV model, the synchronizer PCV model simulates the target valve characteristics well with good linearity, as shown in the ramp-response simulation, and a rise time error of less than 0.01 s.

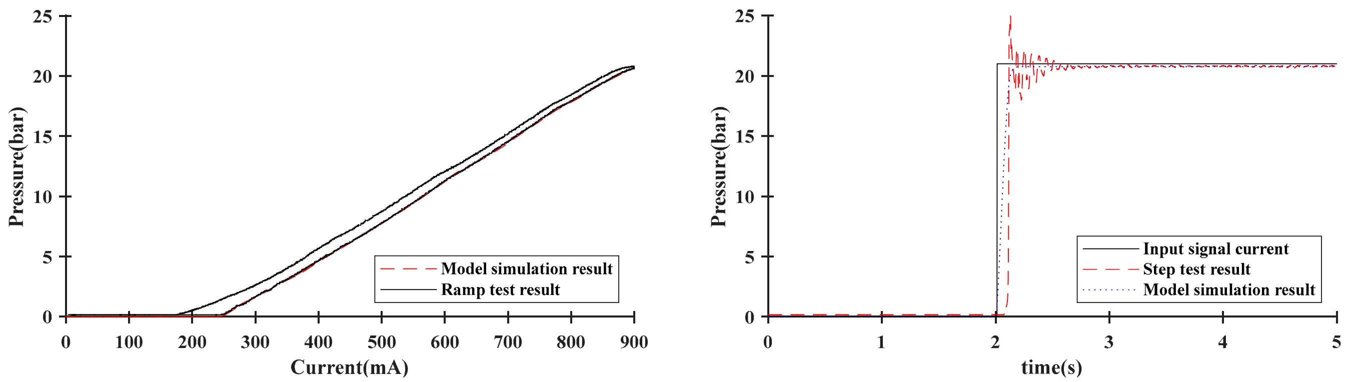

(**a**) (**b**)

Figure 9. Synchronizer PCV model simulation data compared with valve test data: (**a**) Ramp test data; (**b**) Step test data.

The actuator was modeled by reflecting the behavioral characteristics of the target actuator. The 1–3, 2–4, 5–7, and 6–8-stage actuators all had the same behavior characteristics. The sleeve moved 10 mm to the right based on the origin of when the 1st, 2nd, 5th, and 6th stages engaged, and the sleeve moved 10 mm to the left based on the origin of when the 3rd, 4th, 7th, and 8th gear stages were engaged. Figure 10a shows a simple visualization of the target actuator used for the modeling, and Figure 10b shows the operating principle of the actuator. The operating principle using a 1–3 stage synchronizer actuator as an example is described as follows: When the left side was defined as the positive direction based on the origin, the pressure of the 1-stage proportional control valve acted in the negative direction, whereas the pressure of the 3-stage proportional control valve acted in the positive direction. The cross-sectional area to which the pressure of the first-stage proportional control valve was applied was area 3 when the sleeve position was positive and area 2 when it was negative. Equation (1) is the sleeve force when the sleeve position is positive. The cross-sectional area to which the pressure of the 3-stage proportional control valve was applied was area 1 regardless of the sleeve position. Equation (2) shows the sleeve force calculated when the sleeve position is negative.

$$\text{Sleeve position} > 0 : \text{F} = Pressure_1 \times Area_3 - Pressure_3 \times Area_1 \quad (1)$$

$$\text{Sleeve position} < 0 : \text{F} = Pressure_1 \times Area_2 - Pressure_3 \times Area_1 \quad (2)$$

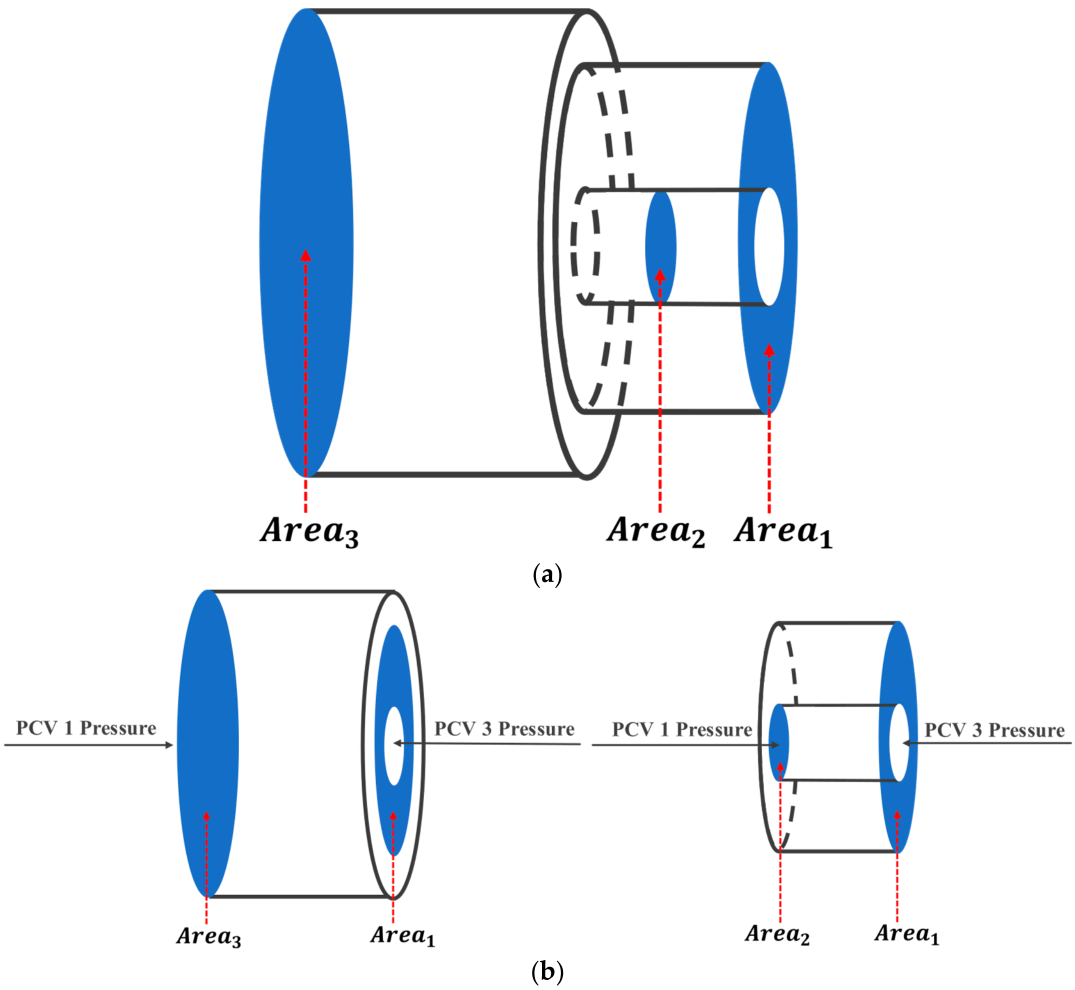

Figure 10. Synchronizer actuator: (**a**) Figure of Synchronizer actuator; (**b**) Mechanism of synchronizer actuator.

When the 1-stage engagement signal current was applied, the 1-stage PCV supplied pressure, and the 3-stage PCV did not. Currently, the sleeve force was negative regardless of the sleeve position from Equations (1) and (2), so the sleeve position converged to −10 mm, and the 1-stage PCV was engaged. When the 3-stage engagement signal current was applied, the 1-stage PCV did not supply pressure, and the 3-stage PCV supplied pressure. Since the sleeve force was positive regardless of the sleeve position according to Equations (1) and (2), the sleeve position converged at +10 mm, and the 3-stage was engaged. When the neutral signal current was applied, the 1-stage PCV and the 3-stage PCV supplied pressure. At this time, the sleeve moved to the origin according to the sleeve force, and the actuator was designed so that the neutral position was engaged by a detent designed around the origin. The actuator was modeled to reflect all the behavioral characteristics of these target actuators at each engagement stage.

Figure 11 shows the synchronizer actuator model that reflects the characteristics of the target PCV and actuator. It was modeled to receive pressure according to the input signal current from the two PCV models, calculate the sleeve force in the actuator model, and supply it to the synchronizer model of 32-speed transmission.

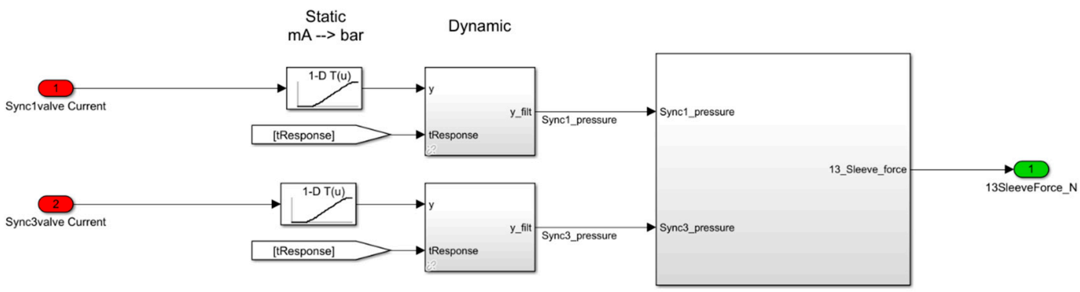

Figure 11. Synchronizer actuator model.

The dog clutch pressure model was modeled, as shown in Figure 12, to supply a large pressure that could engage the manual range shift of the 32-speed transmission per the shift signal directly mechanically provided by the driver.

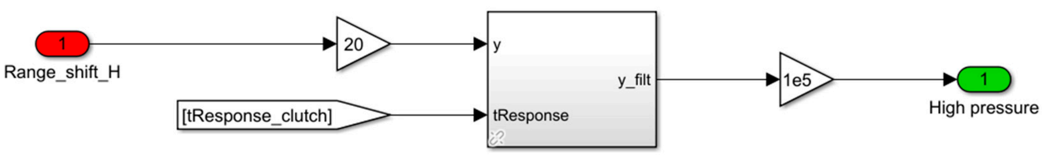

Figure 12. Dog clutch pressure model.

2.4. Engine Modeling

The engine was a module that transmitted rotational power according to the operating mode and target speed. The start motor, RPM control, and torque–RPM map were modeled to implement these engine functions in the tractor model. Figure 13 shows the torque–speed curves of the target engine.

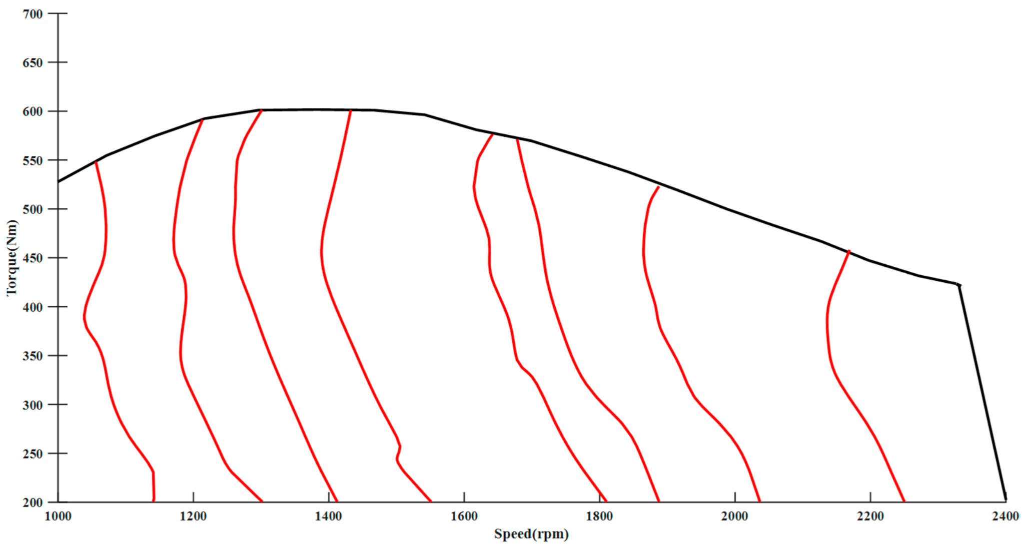

Figure 13. Target engine torque–speed curve.

Figure 14 shows a schematic of the engine model implemented to output torque according to the characteristics of the target engine. The engine's current and target speeds were input, the engine throttle was calculated in the RPM control, and the engine torque was output to the transmission through the current speed and throttle in the torque–RPM map. The start motor assisted the engine torque when the engine start signal was input to start the engine.

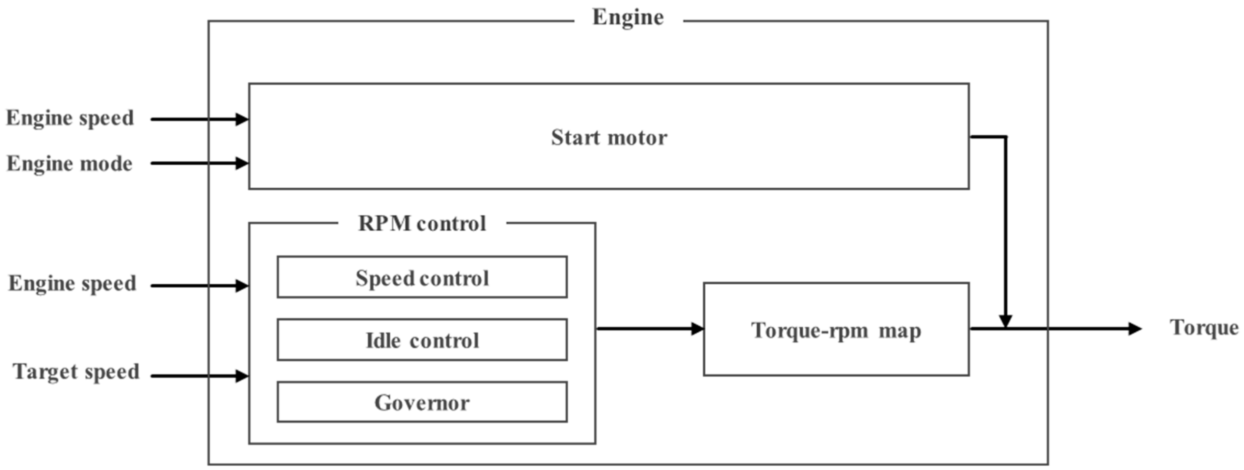

Figure 14. Outline of engine model.

The start motor was modeled, as shown in Figure 15, to reflect the characteristics of the motor so that the engine speed could quickly increase by outputting a torque that was inversely proportional to the engine speed. As shown in Figure 16, the RPM control was modeled to calculate the throttle using three controls: speed control, idle control, and governor control, such that the engine speed reached the target speed. Speed control used proportional–integral–derivative (PID) control to output a throttle for the engine to reach the target speed. Idle control used PID control to output an additional throttle to reach idle RPM when the engine speed was below idle RPM. The governor controlled whether the throttle was open or closed to ensure that the operating point of the engine followed the governor line. PID gain tuning was performed using an optimization function such that the responsiveness of the engine model was similar to that of the target engine. The torque–RPM map was modeled, as shown in Figure 17, to output the engine torque from the torque–RPM curve according to the engine throttle calculated from the RPM control and the current engine speed. In this model, the actual output engine throttle was calculated using a transfer function based on the target engine characteristics, and the torque was output accordingly.

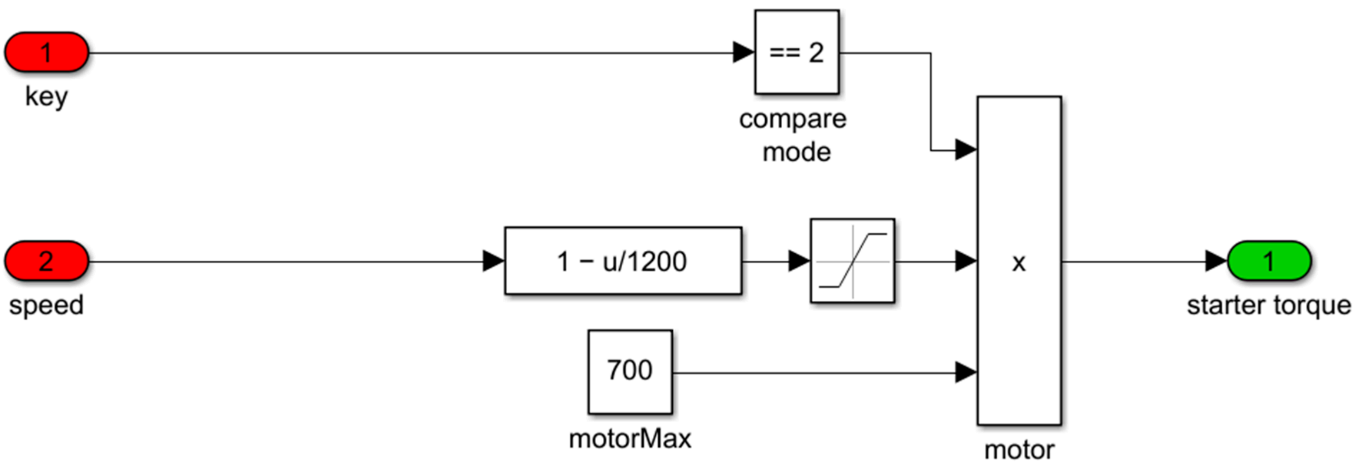

Figure 15. Start motor model.

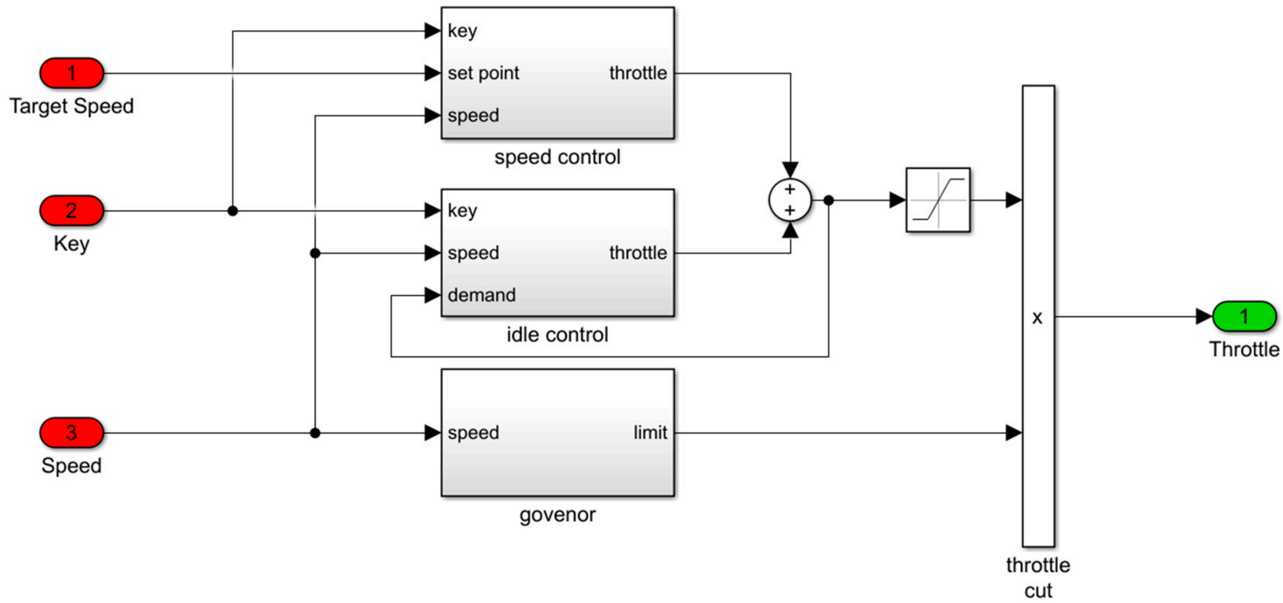

Figure 16. RPM control model.

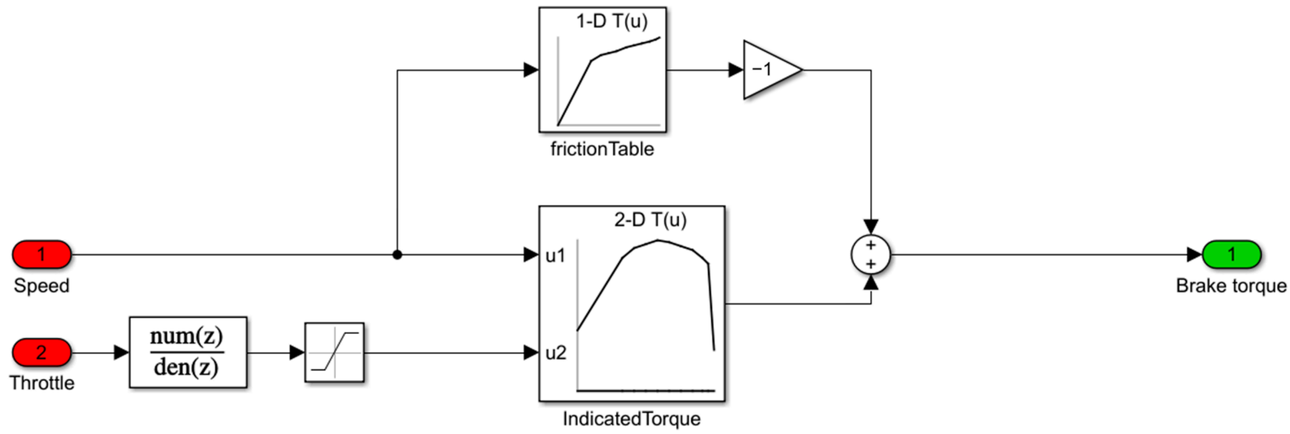

Figure 17. Torque–RPM map model.

2.5. 32-Speed Transmission Modeling

The 32-speed transmission is a module that transmits the rotational power from the engine to the final drive through the power transmission system. The 32-speed gear shift from the automatic 8-speed main gear shift without power interruption through the odd and even clutches and synchronizer and the manual 4-speed sub-shift were configured as shown in Table 5 and implemented in the model. To implement power transmission, the clutch, synchronizer, gear, and shaft were implemented using the Simscape block of MATLAB/Simulink. The clutch was engaged according to the pressure supplied by the HCU and transmitted power to the rear end of the clutch. The model implemented FWD/REV, odd and even clutches, and range-shift H, M, L, and C gear dog clutches. The synchronizer was engaged according to the sleeve force supplied by the HCU and transmitted power to the shaft. Gears and shafts were implemented to transmit power to the final drive of the simple vehicle by engaging the clutch and synchronizer.

Table 5. 32-speed transmission configuration.

●: Engaged	**1**	**2**	**3**	**4**	**5**	**6**	**7**	**8**	**9**	**10**	**11**	**12**	**13**	**14**	**15**	**16**
Sync 1/3	●		●						●		●					
Sync 2/4		●		●						●		●				
Sync 5/7					●		●						●		●	
Sync 6/8						●		●						●		●
Odd clutch	●		●		●		●		●		●		●		●	
Even clutch		●		●		●		●		●		●		●		●
Range creep	●	●	●	●	●	●	●	●								
Range low									●	●	●	●	●	●	●	●
Range middle																
Range high																
	17	18	19	20	21	22	23	24	25	26	27	28	29	30	31	32
Sync 1/3	●		●						●		●					
Sync 2/4		●		●						●		●				
Sync 5/7					●		●						●		●	
Sync 6/8						●		●						●		●
Odd clutch	●		●		●		●		●		●		●		●	
Even clutch		●		●		●		●		●		●		●		●
Range creep																
Range low																
Range middle	●	●	●	●	●	●	●	●								
Range high									●	●	●	●	●	●	●	●

The overall structure of the 32-speed transmission was implemented to be identical to the schematic diagram of the target tractor powertrain. Figure 18 shows a simple schematic of the target tractor powertrain.

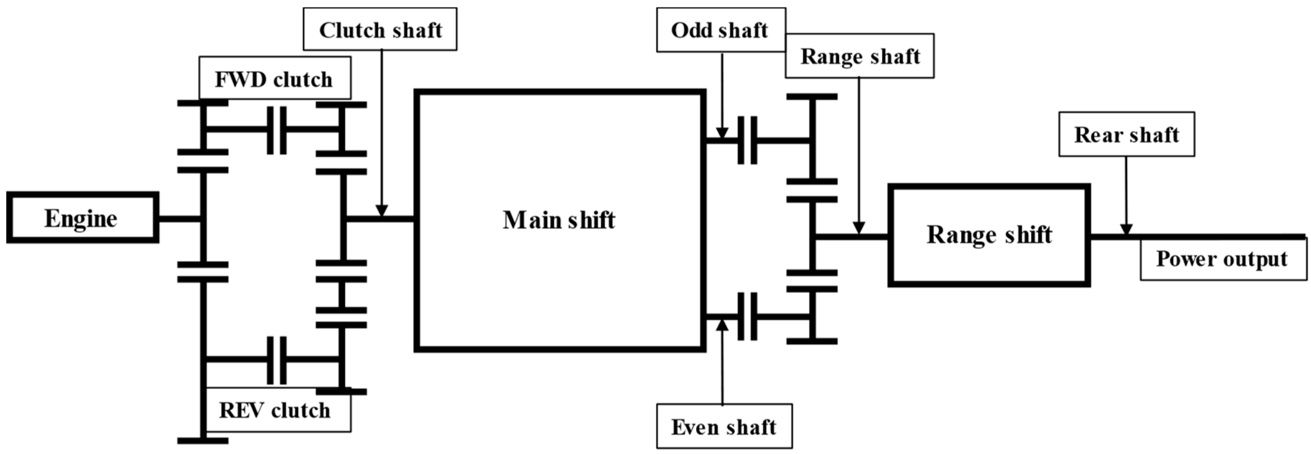

Figure 18. Simple schematic diagram of target tractor powertrain.

The gears and shafts were implemented using simple gear and inertial blocks provided by Simscape. The clutch was modeled to transmit the input engine power to the rear end of the clutch by engaging it according to the clutch pressure determined by the HCU. The clutch model was developed to simulate the clutch reaction force that affected the generated clutch pressure when the clutch chamber was filled with the flow rate supplied by the proportional control valve. The multi-wet clutch system, which was the target clutch of modeling, consisted of a clutch piston, friction plates, oil chamber, and return spring. During the clutch engagement process, the clutch piston moved, and the return spring returned it to its initial position while the oil chamber prevented oil from leaking out. The engine's operating area was different for each operation, and the throttle opening was controlled by the tractor operator using a pedal or hand-throttle lever. Figure 19 shows the clutch model built using the Simscape disk friction clutch block, reflecting the specifications and friction coefficient of the target clutch. The fill and torque phases were implemented based on time and modeled to confirm the shift shock. In the case of 4 manual range shift, it was designed to be engaged/disengaged according to the driver's shift signal through a dog clutch, so it was modeled to receive pressure input from the HCU using the same clutch model. The specifications of the target clutch used in the clutch modeling are listed in Table 6.

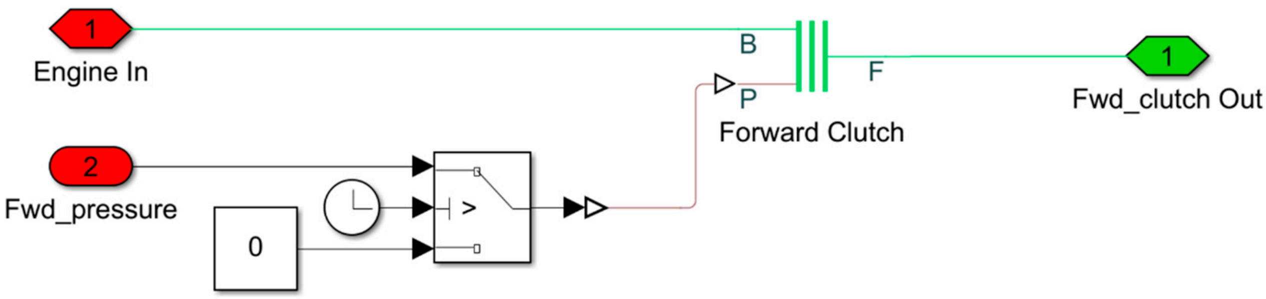

Figure 19. Clutch model.

Table 6. Specification of target clutch used in clutch modeling.

	Number of Disks	Outer Diameter (mm)	Inner Diameter (mm)	Area (mm^2)	Static Friction Coefficient	Kinetic Friction Coefficient
FWD/REV clutch	8	175	120	0.0126	0.1	0.15
Odd/Even clutch	10	178	118	0.0186		

A power transmission simulation confirmed that the clutch model operated correctly. Depending on the input clutch pressure, the model verified that the engagement and power were transmitted to the rear end. The engine power and pressure for clutch engagement were input into the model, and the clutch power transmission was confirmed through a simulation. The power transmission of the clutch was confirmed by comparing the rotational speeds of the front and rear ends of the clutch. Figure 20 shows that the clutch pressure profile entered the clutch simulation. A constant-speed source at 1000 RPM was used for the engine power of the model.

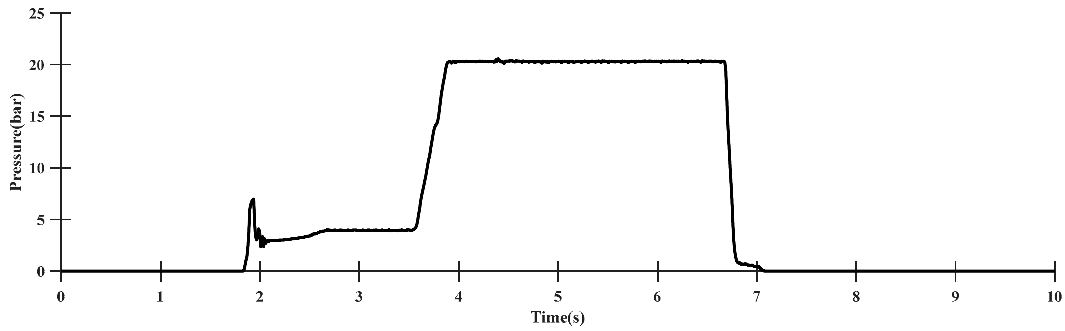

Figure 20. Clutch pressure profile for clutch simulation.

Figure 21 shows the results of the clutch power transmission simulation. The speed before the clutch was the speed at the front end of the clutch. The after speed of the clutch was the speed at the rear end of the clutch. When the clutch pressure profile was entered into the model, power transmission began at t = 2.4 when the fill phase ended. The slope of power transmission increased from t = 3.6 when the proportional control valve was fully filled with hydraulic pressure and clutch engagement began, and at t = 4, when the clutch engagement pressure reached its maximum, the clutch was fully engaged, and the speeds of the front and rear ends of the clutch matched. Thus, it was determined that the power transmission of the clutch model was performed correctly based on the pressure profile.

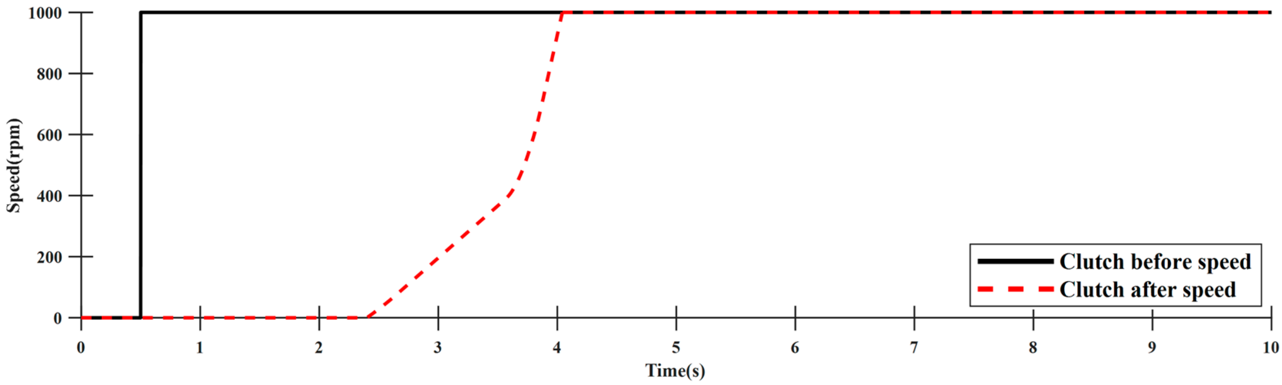

Figure 21. Clutch power transfer simulation result.

Figure 22 shows a synchronizer model built using Simscape blocks to simulate the behavioral characteristics. As an example of a 1–3 stage synchronizer, when the sleeve force of the 1-stage engagement signal was input, the power entering the left gear was transmitted to the hub connected to the odd clutch. When the sleeve force of the 3-stage engagement signal was input, the power entering the right gear was transmitted to the hub connected to the odd clutch. When the sleeve force of the neural signal was input, power was not transmitted to the hub. The synchronizer model was built to transmit power according to the signal inputs.

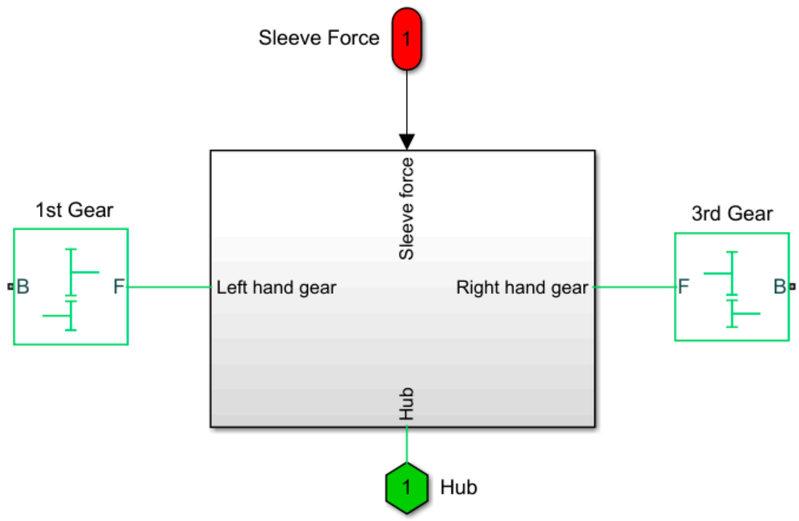

Figure 22. Synchronizer model.

To verify the synchronizer model, the power transmission of the synchronizer shown by the sleeve force input to the synchronizer model was confirmed. Because the synchronization process of the synchronizer model was highly affected by the PCV pressure and the inertia of the front and rear end, the simulation was confirmed; whether its synchronization process has been performed was not investigated in detail. Sleeve force and engine power were input into the synchronizer model. The power transmission when the synchronizer engaged was compared between the rotational speeds of the front end and rear end of the synchronizer. The power transmission when the synchronizer was in neutral was compared with the torque of the front end and rear end of the synchronizer. The sleeve force was entered into the model so that the synchronizer model was 1-stage from 0 to 9 s, 3-stage from 9 to 12.4 s, and neutral from 12.4 s to 20 s.

Figure 23a presents the simulation results when a constant-speed source of 1000 RPM was input as engine power. First gear speed was the speed of the first gear, third gear speed was the speed of the third gear, and the hub speed was the speed of the rear end of the synchronizer connected to the first and third gears. The speed at the synchronizer hub was the same as that at the rear end of 1st gear from 0 to 9 s, and the rear end of 3rd gear from 9 to 20 s meant that 1st and 3rd gears were correctly engaged. Figure 23b shows the simulation results when a constant torque source of 200 Nm was input as the engine power. First gear torque was the torque of the first gear, third gear torque was the torque of the third gear, and hub torque was the torque at the rear end of the synchronizer. The torque at the synchronizer hub was 0 after 12.4 s, which meant that power transmission from both gears was cut off as the synchronizer actuator moved to neutral. According to the simulation results, the synchronizer model was engaged correctly according to the engagement signals of each stage.

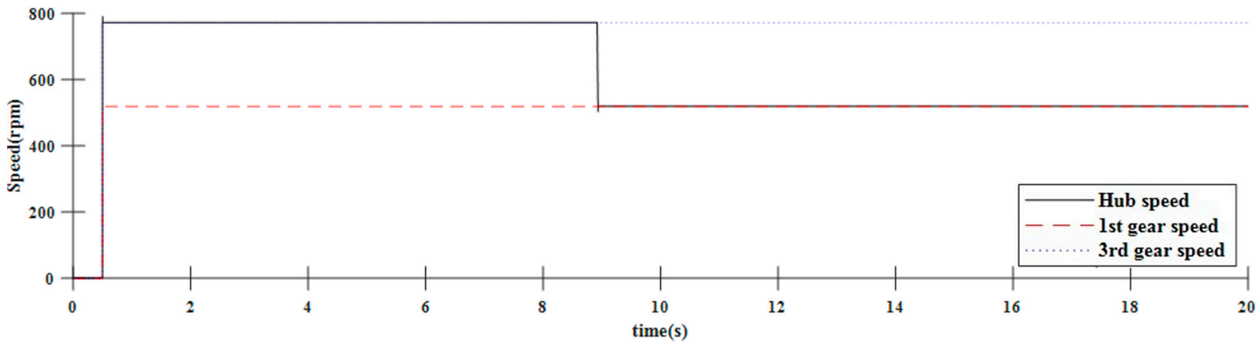

(a)

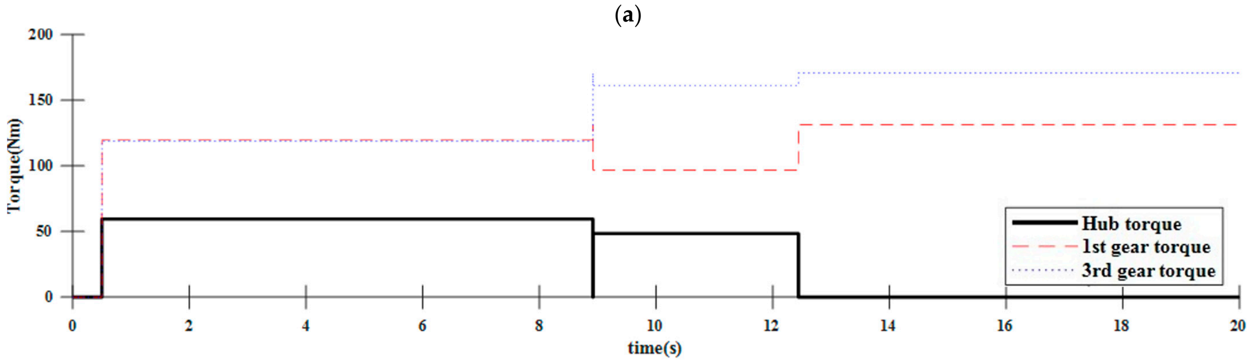

(b)

Figure 23. Synchronizer power transfer simulation result: (**a**) Synchronizer speed transfer simulation result; (**b**) Synchronizer torque tranfer simulation result.

2.6. Simple Vehicle Modeling

A simple vehicle is a dynamic module in which the speed and acceleration of the tractor are determined according to the power transmitted from a 32-speed transmission, and the net force of the tractor is calculated according to the driving state of the tractor. Wheel and vehicle models were constructed to implement the functions of the module. The wheel model was responsible for transmitting the rotational power shifted from the 32-speed transmission of the axle to the linear power of the wheels. The vehicle model calculated the net force and speed through the linear power of the wheels and resistance force.

As shown in Figure 24, the wheel model was built using Simscape's gearset and wheel and axle blocks. The final drive ratio and rear-wheel tire specifications of the target tractor powertrain were reflected in the model. The linear power converted using the wheel model was transferred to the vehicle model to calculate the vehicle speed. The vehicle model shown in Figure 25 comprised a resistance calculation model that determined the net force by calculating the linear power and resistance of the wheels, and a dynamic model that determined the speed by integrating the acceleration. The model calculated resistance through a mathematical model for brake torque input and gradient input. The resistance calculation model calculated the resistance force applied to the vehicle by considering the rolling resistance, drivetrain loss, aerodynamic drag, braking force, and surface gradient under current driving conditions. The braking force F_{Brake} applied to the vehicle due to the brake torque T_B and the wheel radius r_w was calculated using Equation (3). The gradient force $F_{Gradient}$ due to gravity and the angle of the ground θ were calculated using Equation (4). The road load force F_{Load} caused by speed generation were calculated using Equation (5) by adding rolling resistance, drivetrain loss, and aerodynamic drag. Equation (5) is expressed in the zero-order, first-order, and second-order terms of the velocity u, and the coefficients of each term are F_0, F_1, F_2. F_0 is a coefficient related to rolling resistance, F_1 is a coefficient related to rolling resistance and drivetrain loss, and F_2 is a coefficient related to aerodynamic drag. The total resistance force $F_{Resistance}$ applied to the vehicle while driving was calculated using Equation (6). Equation (6) includes not only the resistance generated while driving, but also the force F_{work} generated while the tractor is working.

$$F_{Brake} = T_B \times r_w \tag{3}$$

$$F_{Gradient} = \mathrm{mgsin}(\theta) \tag{4}$$

$$F_{Load} = F_0 + F_1 \times u + F_2 \times u^2 \tag{5}$$

$$F_{Resistance} = F_{Brake} + F_{Gradient} + F_{Load} + F_{Work} \tag{6}$$

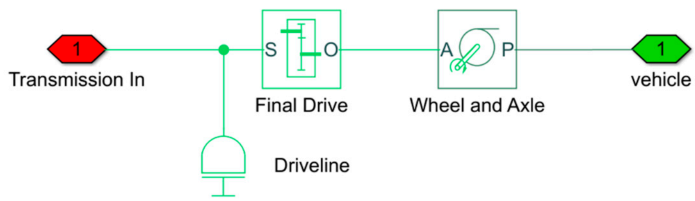

Figure 24. Wheel model.

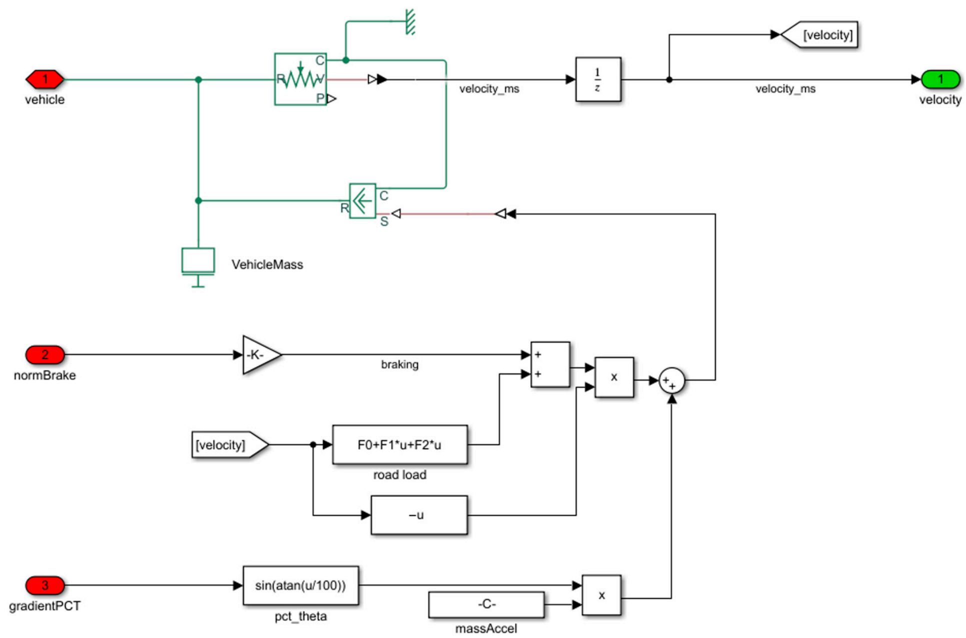

Figure 25. Vehicle model.

The dynamic model calculated the net force F_N, as shown in Equation (7), from the linear force F_{Engine} transmitted from the engine and wheel model and resistance force $F_{Resistance}$ from the resistance calculation model. The output acceleration a and speed v, as shown in Equation (8), from the calculated net force F_N and the mass of tractor $M_{Tractor}$. The dynamic model that determined the vehicle's movement from the calculated net force was composed of an ideal force source block, ideal translational motion sensor block, and mass block.

$$F_N = F_{Engine} - F_{Resistance} \tag{7}$$

$$a = \frac{F_N}{M_{Tractor}},\ v = \int a dt \tag{8}$$

2.7. Plant Model Verification

A tractor-driving simulation was performed to check whether the model accurately reflected the behavior of the target tractor. For the driving simulation, the engine target speed was set to 900 RPM (idle RPM) immediately after starting and 2000 RPM 2 s after starting. The forward clutch was engaged at t = 10 s after starting, and the range gear was maintained in stage M while driving. The main gear was upshifted by 1 from the 1st to 8th gear and downshifted by 1 from the 8th gear to the 1st gear at t = 10–45 s after starting. Figure 26 shows the main shift scenario of the driving simulation. To verify whether the model was running and shifting properly, the behavior of the tractor model was verified by checking the engine speed and throttle according to the main speed, synchronizer, and clutch engagement of the transmission, speed of each shaft of the transmission, and speed of the vehicle.

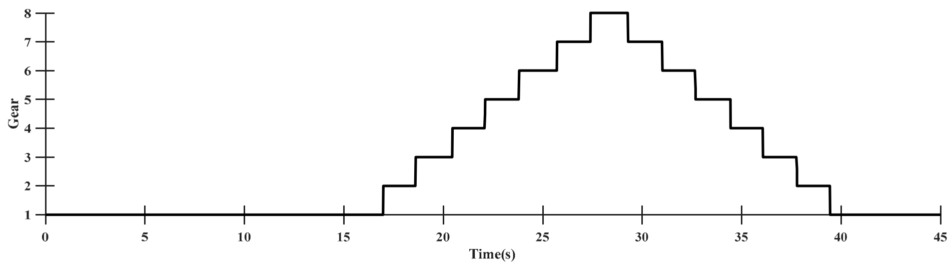

Figure 26. Main shift scenario of model simulation.

Because the purpose of the model was to verify shift performance, it had to be able to express the shock that occurs during shifting. At this time, the shift shock can be confirmed through the change in speed in the vehicle's driving direction because the vehicle model of the simple vehicle submodel was built in one dimension. The shifting performance of the model was verified using the speed change that occurred in the main shift gears during the driving simulation.

3. Results and Discussion

Based on the execution time of the driving simulation, it was confirmed that the model was capable of real-time operation. Table 7 presents the step information for the driving simulation. When the simulation was performed with a fixed step size of 0.001 s, 30.53 s were consumed to run one 45 s simulation. Thus, it was confirmed that the created model could be performed in real time at 1000 Hz.

Table 7. Step information of driving simulation.

Step Information	Value
Solver	Fixed step discrete
Start time	0 s
Stop time	45 s

Table 7. *Cont.*

Step Information	Value
Average step size	1.00×10^{-3}
Total steps	45,000
Run time	30.53 s

The engine speed, throttle, and torque of the simulation confirmed the engine status while driving. Figure 27a shows a graph comparing the engine and target speeds while driving. Figure 27b shows the engine throttle while driving. A graph of engine torque while driving is shown in Figure 27c. The engine torque and throttle were generated to maintain the target speed whenever the target RPM was changed from t = 0 to 4 s. The engine torque and throttle remained constant from t = 4 to t = 10 s when the engine speed reached the target RPM. When the forward clutch was engaged at t = 10 s, the inertia was connected to the rear end of the engine, causing a decrease in speed; however, the target RPM was reached within 1 s because of the torque output according to the RPM control. During the main upshift process, the engine speed decreased owing to fluctuations in the engine throttle and torque caused by the odd/even clutch being alternately engaged and disengaged. It was confirmed that the target RPM was reached through RPM control. When moving from 7th to 8th gear, the engine speed did not reach the target RPM at the maximum throttle, which is believed to be caused by insufficient shift time. During the main downshift process, the engine speed increased owing to fluctuations in the engine throttle and torque and was maintained at the target RPM with RPM control.

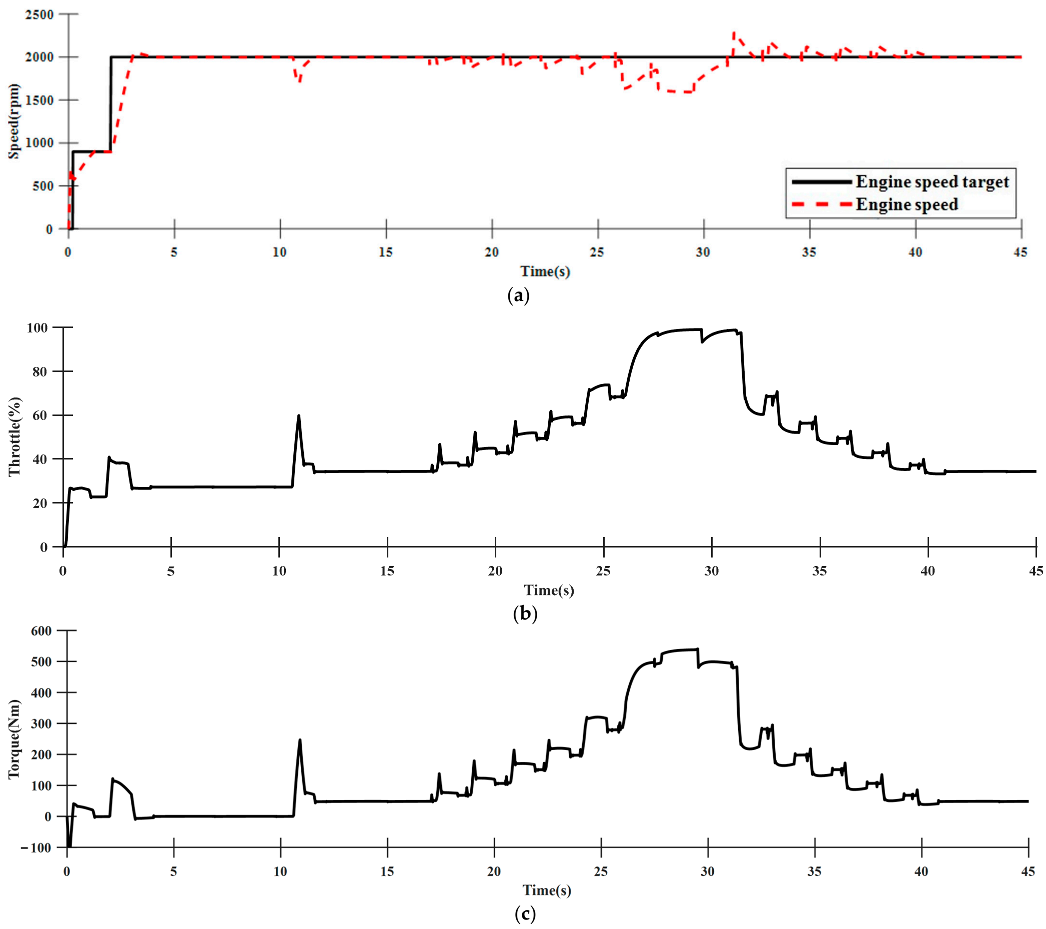

Figure 27. Engine data from full model simulation: (**a**) Engine speed; (**b**) Engine throttle; (**c**) Engine torque.

The power transfer of the 32-speed transmission during the simulation was confirmed by checking the speed of each shaft of the 32-speed transmission, which was engaged according to the clutch pressure and actuator sleeve position. Figure 28a shows a graph of the sleeve position for each synchronizer actuator. Figure 28b shows the forward, odd, and even clutch pressure graphs. Figure 28c shows a graph comparing the speed of each shaft in a 32-speed transmission. The clutch shaft is the rear shaft of the forward clutch and is directly connected to the engine. The odd and even shafts represent the front shafts of the odd and even clutches, respectively. The range shaft is connected to the rear end of the odd/even clutch and is the front shaft of the range shift. The rear shaft was located before the final drive at the rear shaft of the range shift. Immediately after starting, the 1st and 3rd stage synchronizers are in 1-stage, and the odd clutch is engaged. At t = 10 s, the forward clutch is engaged, engine power is transmitted to the shafts, and the speed of each shaft is generated. From the clutch pressure and actuator sleeve position that appeared during the shift progress from t = 10 to 45 s, it was confirmed that the clutch and synchronizer were correctly engaged to generate speed according to the gear ratio required for each shaft of the DCT-type powertrain.

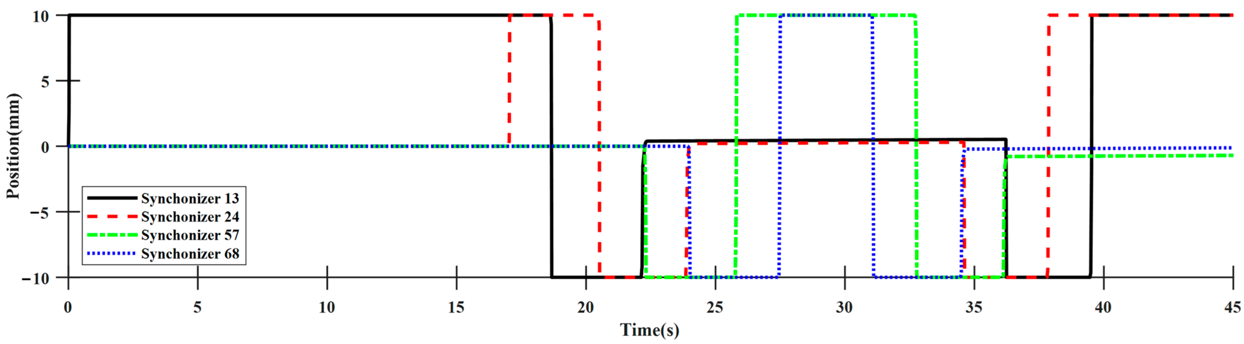

(**a**)

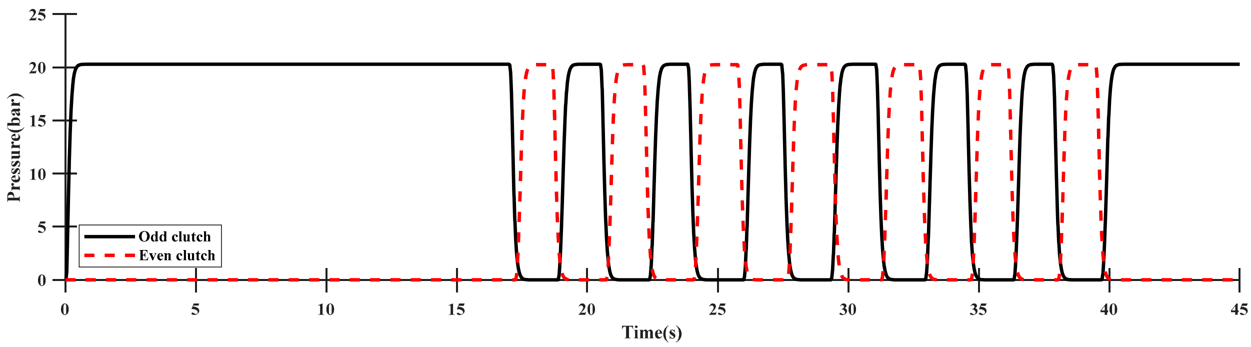

(**b**)

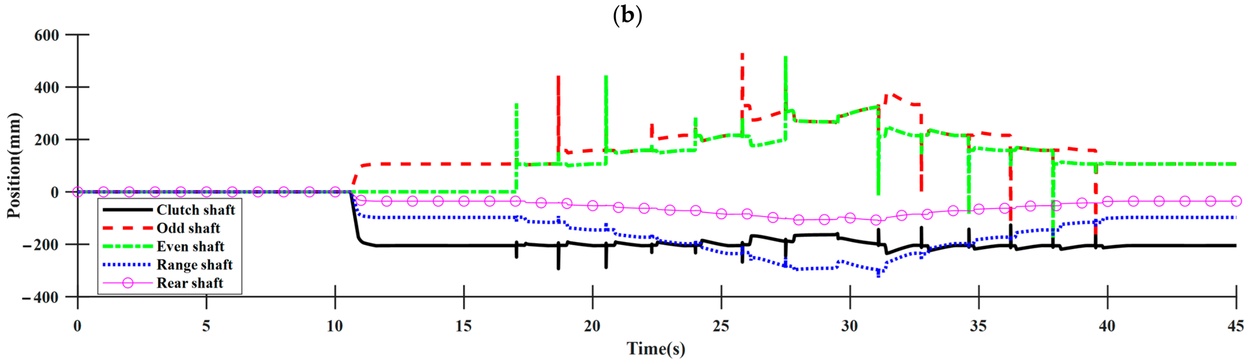

(**c**)

Figure 28. 32-speed transmission data from full model simulation: (**a**) Synchronizer actuator sleeve position; (**b**) Odd/Even clutch pressure; (**c**) Speed of transmission shafts.

The power transmitted from the 32-speed transmission was transmitted to a simple vehicle, and vehicle speed was generated. Figure 29a shows a graph of the vehicle speed calculated using a simple vehicle model. At t = 10 s, the forward clutch was engaged, power was transmitted to the wheels, and the speed was generated by the vehicle model. It was confirmed that the vehicle speed changed according to the designed gear ratio and output owing to the change in shaft speed that occurred as the gear ratio changed according to the main shift from t = 10 to 45 s. In addition, using the developed simulation model, the shock that occurs when shifting gears is confirmed by the acceleration of the vehicle. Figure 29b shows the acceleration graph of the vehicle's driving direction generated through the simulation. An acceleration of up to 3.68 m/s^2 occurred when the forward clutch was first engaged and when the odd/even clutch was alternately engaged/disengaged. In particular, greater acceleration occurred while downshifting rather than while upshifting when shifting in a higher gear rather than a lower gear. Thus, it was confirmed that the model's shift performance requires improvement in higher gears and downshifts.

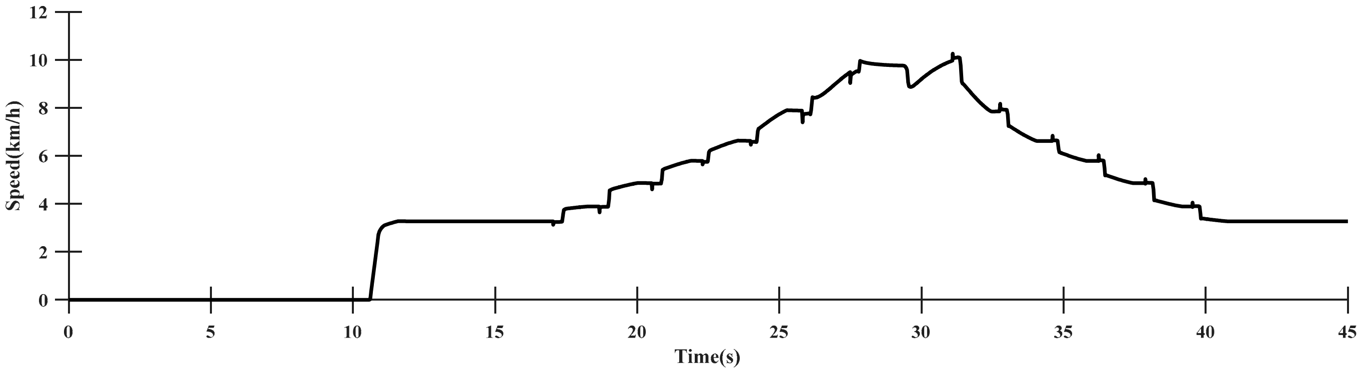

(**a**)

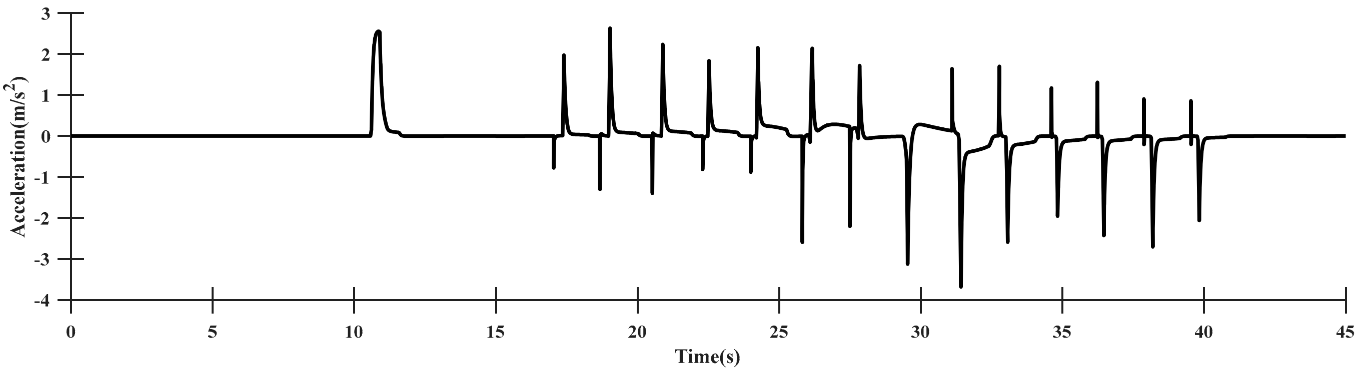

(**b**)

Figure 29. Vehicle speed and acceleration data from full model simulation: (**a**) Vehicle speed; (**b**) Vehicle acceleration.

4. Conclusions

In this study, a real-time tractor simulation model consisting of four submodels was developed to verify shift performance. Among the elements that constitute the HCU model, the clutch PCV, and synchronizer PCV, models were built with the characteristics of the target PCV and verified through ramp-response and step-response simulation. A synchronizer actuator model is constructed to satisfy the behavioral characteristics of the target synchronizer. A dog clutch pressure model was built to supply the pressure at which the range shift clutch could be engaged according to the mechanical input signal. The engine model was built with three elements—the start motor, RPM control, and torque–RPM map—to satisfy the performance of the target engine. The 32-speed transmission model was built with the 32 speeds of a dual-clutch type with an 8-speed main shift and a 4-speed range shift through the clutch, synchronizer, gear, and shaft modeling. The clutch and synchronizer models were verified during the construction. A simple vehicle model was built using the wheel and vehicle models so that the power transmitted from the 32-speed transmission could generate the vehicle's speed.

The full-tractor model was verified using a driving simulation. The execution time of the driving simulation was 30.53 s, which was shorter than the simulation stop time of 45 s, confirming that the simulation could be driven in real time. The engine model followed the target speed well before the forward clutch was engaged. Although fluctuations appeared during the shift process, it was confirmed that the target speed was maintained through RPM control. According to the shifting scenario, the input current to the clutch and synchronizer PCV confirmed that the clutch and synchronizer were normally engaged and disengaged and that the engine power was well transmitted to the final drive. In addition, it was confirmed that the model's driving speed, which appears according to the engine and gear shift speeds, aligns with the designed gear ratio. Therefore, it was determined that the developed plant model satisfied the characteristics of the target tractor and could be used to verify the shift performance. It was confirmed that the shift performance of the developed model was better in the lower gear than in the higher gear and in the upshift than in the downshift.

In addition, the real-time plant model developed in this study serves as a foundation for future advancements. It allows for extensive simulation, including model-in-the-loop and hardware-in-the-loop testing, essential stages in the tractor development process. These simulations aim to verify the performance of the shift control algorithm that replicate the shifting performance by connecting control algorithms to the model. The initial focus on validating the suitability of real-time simulation will be followed by model-in-the-loop testing when the control algorithms are developed. Subsequently, the integration of control algorithms into the hardware will enable comprehensive hardware-in-the-loop testing, marking a significant step toward further development.

Author Contributions: Conceptualization, Y.-J.P. and J.W.L.; Methodology, G.H., D.-V.A., Y.-J.P. and J.W.L.; Investigation, D.-V.A. and D.K.; Validation, G.H. and H.-S.K.; Writing, G.H., Y.-J.P. and J.W.L. All authors have read and agreed to the published version of the manuscript.

Funding: This work was supported by the Technology Innovation Program (20011428, Development of common type dual-clutch transmission system and standardized control platform) funded By the Ministry of Trade, Industry, and Energy (MOTIE, Korea).

Institutional Review Board Statement: Not applicable.

Data Availability Statement: The data presented in this study are available on request from the corresponding author. The data are not publicly available due to the request of the funding of the scientific research projects.

Conflicts of Interest: The authors declare no conflict of interest.

References

1. Cheng, Z.; Lu, Z. Research on the PID control of the ESP system of tractor based on improved AFSA and improved SA. *Comput. Electron. Agric.* **2018**, *148*, 142–147. [CrossRef]
2. Mao, Y.; Wu, Y.; Yan, X.; Liu, M.; Xu, L. Simulation and experimental research of electric tractor drive system based on Modelica. *PLoS ONE* **2022**, *17*, e0276231. [CrossRef]
3. Yiwei, W.; Xianghai, Y.; Zhili, Z. Architecture modeling and test of tractor power shift transmission. *IEEE Access* **2020**, *9*, 3517–3525. [CrossRef]
4. Li, B.; Sun, D.; Hu, M.; Liu, J. Automatic starting control of tractor with a novel power-shift transmission. *Mech. Mach. Theory* **2019**, *131*, 75–91. [CrossRef]
5. Baek, S.Y.; Jung, Y.J.; Ayub, S.M.A.; Nam, K.C.; Kim, T.B.; Choi, C.H.; Kim, Y.-J. Development of simulation model for electric all-wheel-drive tractor. In Proceedings of the 2019 ASABE Annual International Meeting, Boston, MA, USA, 7–10 July 2019; American Society of Agricultural and Biological Engineers: St. Joseph, MI, USA, 2019; p. 1.
6. Kumar, S.; Tewari, V.K.; Bharti, C.K.; Ranjan, A. Modeling, simulation and experimental validation of flow rate of electro-hydraulic hitch control valve of agricultural tractor. *Flow Meas. Instrum.* **2021**, *82*, 102070. [CrossRef]

7. Jeon, C.W.; Kim, H.J.; Yun, C.; Han, X.; Kim, J.H. Design and validation testing of a complete paddy field-coverage path planner for a fully autonomous tillage tractor. *Biosyst. Eng.* **2021**, *208*, 79–97. [CrossRef]
8. Watanabe, M.; Sakai, K. Identifying tractor overturning scenarios using a driving simulator with a motion system. *Biosyst. Eng.* **2021**, *210*, 261–270. [CrossRef]
9. Mocera, F. A model-based design approach for a parallel hybrid electric tractor energy management strategy using hardware in the loop technique. *Vehicles* **2020**, *3*, 1–19. [CrossRef]
10. Bélanger, J.; Venne, P.; Paquin, J.N. The what, where and why of real-time simulation. *Planet Rt* **2010**, *1*, 25–29.
11. Ruan, S.; Ma, Y.; Yang, N.; Xiang, C.; Li, X. Real-time energy-saving control for HEVs in car-following scenario with a double explicit MPC approach. *Energy* **2022**, *247*, 123265. [CrossRef]
12. Tamás, G.; Fodorean, D. Model in the loop simulation of an electric propulsion system using virtual reality. In Proceedings of the 2017 52nd International Universities Power Engineering Conference (UPEC), Heraklion, Greece, 28–31 August 2017.
13. Moten, S.; Celiberti, F.; Grottoli, M.; van der Heide, A.; Lemmens, Y. X-in-the-loop advanced driving simulation platform for the design, development, testing and validation of ADAS. In *2018 IEEE Intelligent Vehicles Symposium (IV)*; IEEE: Piscataway, NJ, USA, 2018.
14. Abdelrahman, A.S.; Algarny, K.S.; Youssef, M.Z. A novel platform for powertrain modeling of electric cars with experimental validation using real-time hardware in the loop (HIL): A case study of GM second generation Chevrolet volt. *IEEE Trans. Power Electron.* **2018**, *33*, 9762–9771. [CrossRef]
15. Aksjonov, A.; Ricciardi, V.; Augsburg, K.; Vodovozov, V.; Petlenkov, E. Hardware-in-the-loop test of an open-loop fuzzy control method for decoupled electrohydraulic antilock braking system. *IEEE Trans. Fuzzy Syst.* **2020**, *29*, 965–975. [CrossRef]
16. Parra, A.; Rodriguez, A.J.; Zubizarreta, A.; Perez, J. Validation of a real-time capable multibody vehicle dynamics formulation for automotive testing frameworks based on simulation. *IEEE Access* **2020**, *8*, 213253–213265. [CrossRef]
17. Moreno, I.J.; Ouardani, D.; Chaparro-Arce, D.; Cardenas, A. Real-Time Hardware-in-the-Loop Emulation of Path Tracking in Low-Cost Agricultural Robots. *Vehicles* **2023**, *5*, 894–913. [CrossRef]
18. Liu, Y.; Huang, B.; Yang, Y.; Lei, Z.; Zhang, Y.; Chen, Z. Hierarchical speed planning and energy management for autonomous plug-in hybrid electric vehicle in vehicle-following environment. *Energy* **2022**, *260*, 125212. [CrossRef]
19. Yang, B.; Guo, L.; Ye, J. Real-time simulation of electric vehicle powertrain: Hardware-in-the-loop (HIL) testbed for cyber-physical security. In Proceedings of the 2020 IEEE Transportation Electrification Conference & Expo (ITEC), Chicago, IL, USA, 23–26 June 2020; IEEE: Piscataway, NJ, USA, 2020; pp. 63–68.
20. Shen, W.; Zhang, Q.; Chen, Z.; Mao, W.; Li, Y. Testing and analysis of automotive gearshift performance based on gear shift analysis. *Eng. Rep.* **2021**, *3*, e12324. [CrossRef]
21. Wu, P.; Qiang, P.; Pan, T.; Zang, H. Multi-objective optimization of gear ratios of a seamless three-speed automated manual transmission for electric vehicles considering shift performance. *Energies* **2022**, *15*, 4149. [CrossRef]
22. He, B.; Chen, Y.; Wei, Q.; Wang, C.; Wei, C.; Li, X. Performance Comparison of Pure Electric Vehicles with Two-Speed Transmission and Adaptive Gear Shifting Strategy Design. *Energies* **2023**, *16*, 3007. [CrossRef]
23. Park, J.; Choi, S. Gear shifting based on MIMO model predictive control for convenient adjustment of shifting performance. *IEEE Trans. Veh. Technol.* **2021**, *71*, 233–249. [CrossRef]
24. Schmiedt, M.; He, P.; Rinderknecht, S. Target state optimization: Drivability improvement for vehicles with dual clutch transmissions. *Appl. Sci.* **2022**, *12*, 10283. [CrossRef]
25. Huang, W.; Zhang, J.; Huang, J.; Yin, C.; Wang, L. Optimal speed regulation control of the hybrid dual clutch transmission shift process. *World Electr. Veh. J.* **2020**, *11*, 11. [CrossRef]
26. Milindar, S.D.; Prasanna, S.; Baskar, P. Comprehensive review on dual clutch transmission. *Int. J. Veh. Perform.* **2022**, *8*, 74–108. [CrossRef]
27. Li, A.; Qin, D. Adaptive model predictive control of dual clutch transmission shift based on dynamic friction coefficient estimation. *Mech. Mach. Theory* **2022**, *173*, 104804. [CrossRef]
28. Guo, J.; Zhang, Y. Adaptive Starting Control Strategy for Hybrid Electric Vehicles Equipped with a Wet Dual-Clutch Transmission. *Actuators* **2023**, *12*, 123. [CrossRef]
29. Song, X.; Liu, J.; Smedley, D. Simulation study of dual clutch transmission for medium duty truck applications. *SAE Int. J. Commer. Veh.* **2005**, *114*, 264–270.
30. Galvagno, E.; Velardocchia, M.; Vigliani, A. Dynamic and kinematic model of a dual clutch transmission. *Mech. Mach. Theory* **2011**, *46*, 794–805. [CrossRef]